Precise Fault Location Detection for 400kV Overhead Transmission Lines and Underground Cables

Project Report

Jay David Crozier

Aalborg University

Electrical Power Systems and High Voltage

AALBORG UNIVERSITY
STUDENT REPORT

AAU Energy
Aalborg University

Title:
Precise Fault Location Detection for 400kV Overhead Transmission Lines and Underground Cables
Theme:
Electrical Power System

Project Period:
Fall Semester 2025

Participant(s):
Jay David Crozier

Supervisors:
Sanjay Chaudhary
Hanchi Zhang

Copies: 1

Page Numbers: [34]

Date of Completion:
January 9th, 2026

The transition of the Danish transmission grid towards underground cabling creates hybrid lines composed of alternating overhead line (OHL) and underground cable (UGC) segments. This topology complicates fault localisation by disrupting the linear impedance-distance relationship utilised by conventional impedance-based protection. This thesis evaluates a Two-Terminal Synchronised Travelling Wave (TW) algorithm as an alternative for accurate fault localisation on Energinet's planned 400 kV Kassø-Landerupgård connection. A detailed electromagnetic transient model was developed in PSCAD utilising frequency-dependent phase models to replicate the complex wave propagation behaviour within cross-bonded XLPE cables. The investigation assesses the hypothesis that a single "System Effective Velocity" is sufficient to linearise the fault calculation across the heterogeneous medium. While the algorithm successfully identified wavefront arrivals despite attenuation at OHL-UGC interfaces, the results demonstrate that a single calibrated velocity yields a location error of approximately 3% for remote faults. This discrepancy arises because the total propagation time is strictly dependent on the specific lengths of OHL and cable traversed rather than a constant system average. Consequently, the study concludes that achieving metre-level accuracy requires a segmented velocity profile that adapts to the specific fault zone rather than relying on a uniform velocity assumption.

Summary

The ongoing expansion of the Danish transmission grid involves the integration of extensive underground cable (UGC) sections into the existing 400 kV overhead line (OHL) network. This development creates hybrid transmission lines characterised by severe impedance discontinuities at the transition points. These discontinuities disrupt the linear reactance-distance relationship relied upon by conventional distance protection, rendering standard fault location methods inaccurate.

This project investigates the viability of a Two-Terminal Synchronised Travelling Wave (TW) fault location algorithm as a precision alternative for Energinet's planned Kassø-Landerupgård connection. The main objective is to determine if a passive travelling wave method can achieve accurate fault location across a heterogeneous medium.

A high-fidelity electromagnetic transient model of the planned hybrid system topology was developed in PSCAD. The model incorporates the Frequency-Dependent (Phase) model to accurately simulate the skin effect and complex wave propagation behaviour within the cross-bonded XLPE cable sections. The study evaluates a "System Effective Velocity" method, where a single average propagation velocity is calibrated from a reference fault event and applied to locate faults in other segments of the hybrid system.

Simulation results demonstrate that the hybrid topology does not prevent the transmission of the initial fault transient, although significant attenuation occurs at the OHL-UGC interfaces. The algorithm successfully detected wavefront arrivals at both terminals with microsecond-level precision. However, the validation scenarios revealed a fundamental limitation in the single average propagation velocity hypothesis. While the system was calibrated successfully for a local zone (0% error), applying this single effective velocity to a remote fault resulted in a location error of approximately 3.1% (2.3 km).

The analysis concludes that this error arises from the velocity dispersion inherent in the hybrid line. Since the propagation velocity in overhead lines differs significantly from that in cables, the "average" velocity is strictly dependent on the specific length of OHL and UGC the wave traverses. As the ratio of OHL to UGC distances changes depending on the fault location, a single calibrated velocity becomes invalid for remote zones. To achieve precise fault localisation, it is recommended that the protection logic adopts a segmented velocity map, applying specific propagation constants corresponding to the distinct OHL and UGC zones identified by the algorithm.

Contents

Preface

Aalborg University, January 9, 2026

This Master's thesis was prepared during the 3rd and 4th semesters of the Master of Science programme in Electrical Power Systems and High Voltage Engineering at Aalborg University.

The project is based on a problem formulation proposed by Energinet, addressing the operational difficulty of locating faults within the underground cable sections of hybrid transmission lines. Currently, identifying the exact location of a cable fault often requires time-consuming physical site inspections. Consequently, this thesis investigates a precise fault location method to mitigate this operational challenge.

The report is written for engineers and researchers within the field of electrical power systems. It is assumed that the reader possesses a fundamental knowledge of power system protection, electromagnetic transients, and high-voltage engineering.

I would like to thank my supervisors, Sanjay Chaudhary and Hanchi Zhang, for their guidance and feedback throughout the project period.

I would also like to extend my gratitude to Søren Damsgaard Mikkelsen (Project Director, National Strategic Projects at Energinet). His proposal of this specific topic and provision of basic technical parameters for the planned Kassø-Landerupgård connection were fundamental to the creation of the simulation model and the relevance of this study.

Jay David Crozier

<jcrozi23@student.aau.dk>

Glossary

AC	Alternating Current
CIGRE	International Council on Large Electric Systems
DC	Direct Current
EMT	Electromagnetic Transient
EMTR	Electromagnetic Time Reversal
GPS	Global Positioning System
HDPE	High-Density Polyethylene
HV	High Voltage
HVAC	High Voltage Alternating Current
OHL	Overhead Line
OPGW	Optical Ground Wire
PSCAD	Power Systems Computer Aided Design
TDR	Time Domain Reflectometry
TEM	Transverse Electro-Magnetic
TSO	Transmission System Operator
TW	Travelling Wave
UGC	Underground Cable
UHF	Ultra-High Frequency
UTC	Coordinated Universal Time
XLPE	Cross-linked Polyethylene

Chapter 1

1. Introduction

1.1 Background

The European energy landscape is undergoing a fundamental transformation driven by the imperative to decarbonise the power sector. Denmark, as a frontrunner in this transition, has committed to an ambitious goal of a 100% renewable energy supply. This shift necessitates a robust expansion of the transmission grid to integrate remote generation sources, particularly offshore wind farms.

Historically, high-voltage power transmission has relied on overhead lines (OHL) due to their technical maturity and cost-effectiveness. However, public acceptance of new transmission infrastructure has become a defining constraint for Transmission System Operators (TSOs). In response to public concerns regarding visual pollution and land value depreciation, the Danish Parliament adopted the "Cable Action Plan" (Kabellægningsplanen) [6]. While this mandate forces the undergrounding of many 132 kV and 150 kV grids, fully undergrounding the 400 kV backbone remains technically and economically challenging due to high capacitive charging currents and the need for extensive reactive power compensation.

To balance these sociopolitical constraints with technical feasibility, Energinet has adopted a hybrid transmission topology. These lines consist of existing or new OHL sections alternating with segments of underground cables (UGC) in environmentally sensitive or populated areas [5]. While this solution addresses public concern, it introduces significant complexity to the protection and control systems.

1.2 Problem Statement

Hybrid transmission lines create a non-homogeneous impedance profile where the characteristic impedance rises sharply from around 30-50 ohms in XLPE cables to approximately 300-400 ohms in overhead lines. These abrupt changes at transition stations create reflection points for electromagnetic waves. Additionally, the necessary cross-bonding of cable sheaths introduces periodic impedance discontinuities that further disperse the fault signal [2, 12].

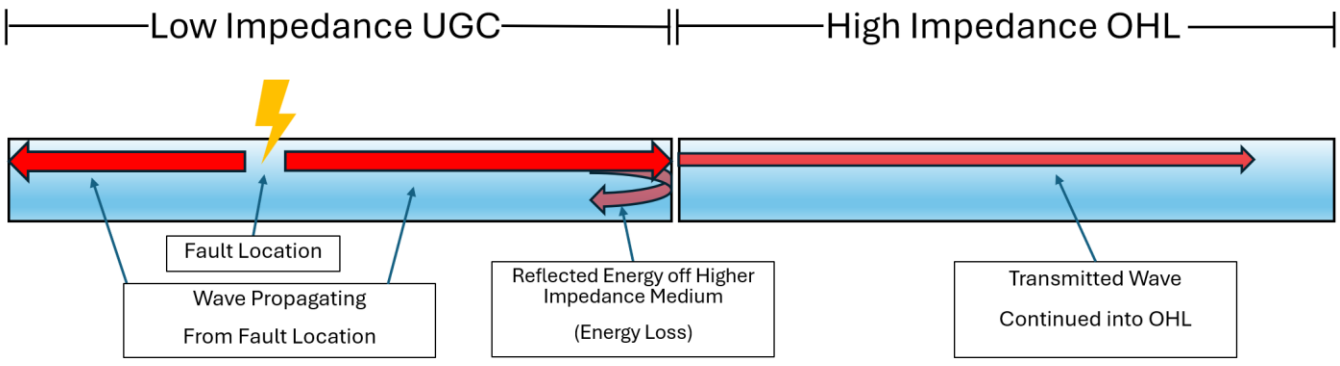

Figure 1.1: Illustration of Impedance Mismatch Reflections at the UGC-OHL Transition

Moreover, the substantial capacitance of the cable sections generates charging currents that distort the measurements seen by protection relays, causing conventional impedance-based methods to fail in determining the fault location accurately [1, 9]. This technical gap leads to the following research question:

How can a Two-Terminal Synchronised Travelling Wave fault location algorithm be designed and simulated to accurately pinpoint faults on the Kassø-Landerupgård hybrid line, despite system heterogeneity and sheath cross-bonding effects?

1.3 Project Objective

The main objective of this thesis is to investigate, develop, and validate the Two-Terminal Synchronised Travelling Wave (TW) method for precision fault location on the Energinet Kassø to Landerupgård hybrid transmission line.

The specific tasks are:

1. To develop a high-fidelity Electromagnetic Transient (EMT) model of the hybrid OHL/UGC system in PSCAD, correctly defining the geometry and implementing the Frequency-Dependent (Phase) Model required for accurate wave propagation analysis [9, 11].
2. To analyse the propagation characteristics of the coaxial travelling wave across the multiple OHL/UGC junctions and assess the hypothesis that a single "System Effective Velocity" can sufficiently linearise the fault location calculation across the heterogeneous topology.
3. To investigate the method's performance by simulating faults at various locations across the OHL and UGC sections of the model, testing under multiple fault scenarios.
4. To determine the fault distance by applying the established TW calculation to the transient current signals measured at the synchronised line terminals [3].
5. To conduct a performance analysis of the method, verifying the achieved fault location accuracy against the known simulated fault position and quantifying the dispersion error introduced by the non-homogeneous medium.

1.4 Scope and Limitations

This project specifically focuses on the design and simulation of the fault location algorithm for the UGC sections of the 400 kV hybrid topology. While the algorithm is theoretically applicable to the entire line, fault location on OHL is considered a technically mature field with established impedance-based solutions. In contrast, remote fault location within hybrid UGC sections remains a significant technical challenge due to impedance discontinuities. Therefore, the simulation scenarios are explicitly targeted at validating fault locating performance within the cable segments of the hybrid system. The scope is limited to ideal fault inception using a timed breaker and assumes perfectly synchronised measurement units (such as GPS-based units) at both terminals, as the PSCAD simulation environment operates on a unified time base. The project does not include the physical design of the monitoring hardware, the impact of current/voltage transformer frequency response, or the complexities of data communication latency between terminals.

1.5 Thesis Outline

The report is structured to guide the reader through the theoretical basis, modelling methodology, and validation of the proposed fault location algorithm.

- **Chapter 2: State of Art** reviews the fundamental challenges of protection in hybrid networks and evaluates the limitations of conventional impedance-based and single-terminal travelling wave methods. It establishes the theoretical justification for adopting a two-terminal synchronised approach.
- **Chapter 3: Methodology** details the construction of the high-fidelity electromagnetic transient model in PSCAD. It defines the specific system topology, the frequency-dependent cable parameters, and the mathematical derivation of the "System Effective Velocity" used for calibration.
- **Chapter 4: Simulation Results** presents the experimental data obtained from the simulation model. It analyses the algorithm's performance across different fault scenarios, quantifying the accuracy and identifying the impact of signal attenuation and dispersion.
- **Chapter 5: Discussion and Conclusion** synthesises the findings, discussing the physical causes of the observed velocity dispersion errors. It concludes with an evaluation of the method's viability for the Energinet grid and provides recommendations for future implementation strategies.

Chapter 2

2. State of Art

2.1 Challenges in Fault Location in Hybrid Systems

Fault location in transmission systems is fundamental to grid reliability. Rapid identification of the fault site allows maintenance crews to repair damage swiftly, minimising downtime and reducing maintenance expenditure [2]. In homogeneous lines (pure OHL), the relationship between impedance and distance is linear. In hybrid lines, this linearity is broken. The different surge impedances of cables and overhead lines cause the voltage and current phasors to behave non-linearly along the line length. Additionally, the capacitive current injection from the cables confuses the reactance measurement algorithms used in standard distance relays [12].

Furthermore, the operational procedure for fault restoration in hybrid lines distinguishes between 'prelocation' and 'pinpointing'. Faults within underground cable sections, particularly those with extruded XLPE insulation, frequently exhibit high-resistance characteristics after the line trips. In the field, detecting these faults often requires 'conditioning' the cable with high-voltage impulses (such as the Surge Arc Reflection Method) to re-ignite the arc for detection by local equipment [2]. This process is time-consuming and stresses the insulation. Consequently, this thesis investigates a precision 'prelocation' method based on the initial fault transient. By accurately estimating the fault distance remotely, the search area for on-site pinpointing teams is reduced, eliminating the need for extensive patrolling or conditioning along the cable route.

2.2 Conventional Fault Location Methods

2.2.1 Impedance-Based Methods

Standard distance protection calculates the impedance to the fault (Z_f) using the fundamental frequency (50 Hz) voltage and current. While robust for standard lines, this method suffers in hybrid applications due to the "shunt capacitance effect." The large charging current of the cable flows through the line but not into the fault, causing the relay to under-reach or over-reach depending on the fault location relative to the cable section [1].

2.2.2 Single-Terminal Travelling Wave Methods

Early TW methods attempted to locate faults using a single terminal by measuring the time between the initial surge arrival and the subsequent reflection from the fault ($t_{reflection} - t_{initial}$). In hybrid lines, this is problematic because the transition points (OHL-UGC junctions) act as reflectors. A single-ended relay struggles to distinguish between the reflection from the fault and the reflection from a normal transition compound, leading to erroneous results [5, 14].

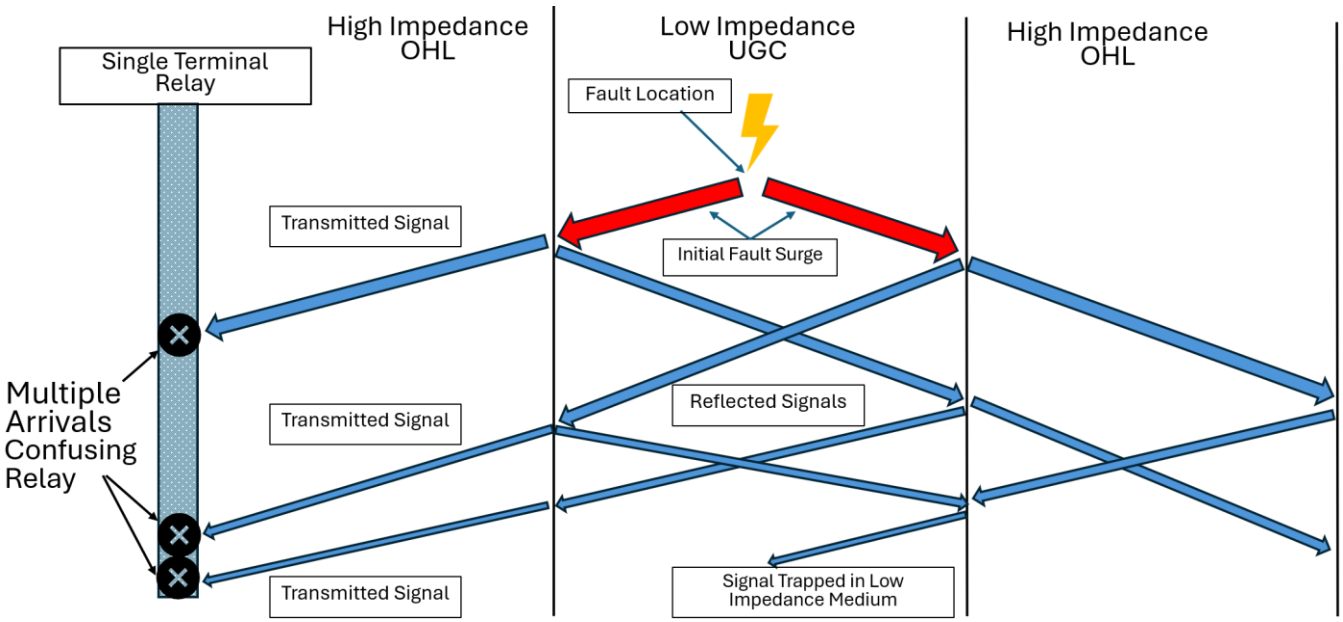

Figure 2.1: Illustration of Multiple Signal Reflections Causing Clutter in a Hybrid Line

2.3 Chosen Methodology: Two-Terminal Synchronised Travelling Wave (TW) Method

To overcome the limitations of impedance and single-ended methods, this project employs a two-terminal synchronised approach. By utilising global positioning system (GPS) time stamping, relays at both ends of the line (Kassø and Landerupgård) can record the absolute arrival time of the fault surge [3]. This method avoids the reliance on conventional impedance estimation, relying instead on the signal propagation velocity and precise differential arrival times of the fault transient. Consequently, the internal reflections at transition compounds, which confuse single-ended methods, can be ignored as the algorithm focuses only on the first incident wavefront arriving at each terminal.

2.4 Physics of Propagation in Hybrid Media

The success of the TW method depends on the accurate estimation of propagation velocity. Wave propagation on a transmission line is governed by the Telegrapher's Equations, which describe the voltage and current distribution along the line [7]:

$$\frac{dV}{dx} = -(R + jwL) * I \qquad (2.1)$$

$$\frac{dI}{dx} = -(G + jwC) * V \qquad (2.2)$$

Where:

- R is resistance (ohms/m)
- L is inductance (H/m)
- G is conductance (S/m)

- C is capacitance (F/m)

2.4.1 Characteristic Impedance and Velocity

For high-frequency travelling waves, the resistive losses (R) and conductance (G) are often negligible compared to the inductance and capacitance. The Characteristic Impedance (Zc) is defined as [7]:

$Z_c = \text{sqrt}(\frac{L}{C})$ (2.3)

The propagation velocity (v) is determined by the inverse square root of the inductance and capacitance [7]:

$v = \frac{1}{\text{sqrt}(L * C)}$ (2.4)

2.4.2 Propagation Differences

- **Overhead Lines:** The electromagnetic field propagates primarily in air, ε_r (epsilon$_r$ approx. 1.0), resulting in a velocity near the speed of light (c approx. 3.0 * 10^8 m/s) [7].
- **Underground Cables:** The field is confined within the XLPE insulation (ε_r approx. 2.3). Since velocity is inversely proportional to the square root of permittivity (v proportional to 1 / sqrt(ε_r)), the wave travels significantly slower in the cable sections [8].
- **Cross-Bonding:** Long HV cables use cross-bonding to cancel sheath currents. These bonding points represent minor impedance discontinuities which can cause signal attenuation and dispersion, a factor that must be accounted for in the simulation model [12].

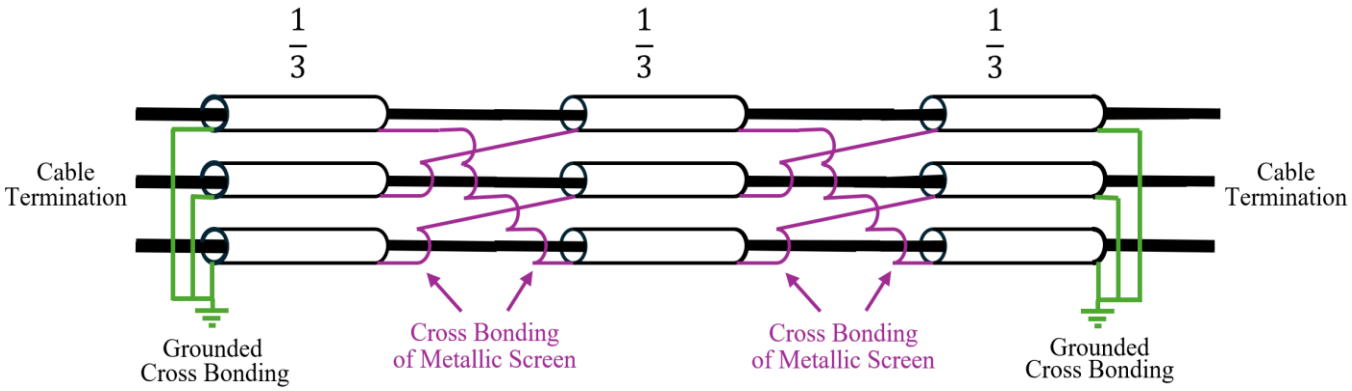

Figure 2.2: Configuration of Sheath Cross-Bonding

2.5 Summary

This chapter reviewed the fundamental limitations of impedance-based protection when applied to hybrid transmission topologies. The literature indicates that impedance discontinuities at OHL-UGC interfaces disrupt the linear reactance-distance relationship, rendering single-ended methods unreliable. Consequently, the Two-Terminal Synchronised Travelling Wave method was identified as the theoretical alternative for investigation. This approach utilises the physics of high-frequency wave propagation to bypass the limitations of power-frequency reactance measurements.

Chapter 3

3. Methodology

The methodology relies on the precise modelling of electromagnetic transients in PSCAD and the application of a passive two-terminal location algorithm. This chapter outlines the system topology, the simulation parameters, and the mathematical framework used for fault location.

3.1 System Topology

The modelled system represents a specific 400 kV connection within the Energinet transmission grid, extending from Kassø to Landerupgård. This line is characterised by a heterogeneous composition of overhead lines (OHL) and underground cables (UGC), creating a discontinuous impedance profile.

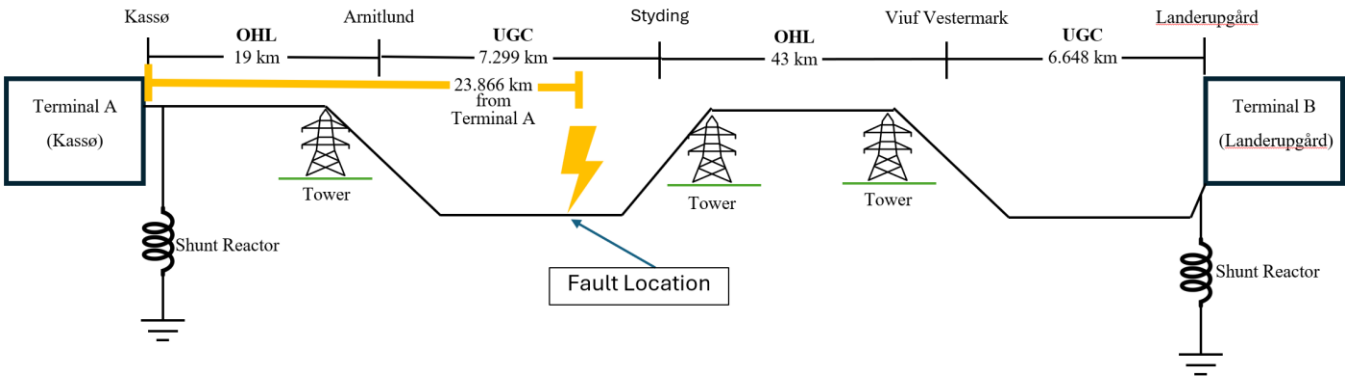

Figure 3.1: Overview of Kassø-Landerupgård Hybrid Transmission Line Topology

The total path length is 75.947 km, divided into four distinct sections:

1. **Kassø to Arnitlund:** A 19.0 km overhead line section.
2. **Arnitlund to Styding:** A 7.299 km underground cable section. To mitigate sheath circulating currents, this section is cross-bonded into three minor sections of 2.433 km each.
3. **Styding to Viuf Vestermark:** A 43.0 km overhead line section.
4. **Viuf Vestermark to Landerupgård:** A 6.648 km underground cable section, cross-bonded into three minor sections of 2.216 km each.

The alternating nature of these sections (OHL-UGC-OHL-UGC) introduces multiple reflection points (acoustic impedance mismatches) that traditional impedance-based relays struggle to interpret correctly.

3.2 Simulation Modelling

The system was modelled using PSCAD to capture high-frequency transients [11].

3.2.1 Cable Modelling

The **Frequency-Dependent (Phase) Model** was selected for the cables rather than the simpler Bergeron model. The Bergeron model assumes constant parameters at a single frequency (50 Hz), which is insufficient for travelling wave analysis where the wavefront contains frequencies in the MHz range. The Frequency-Dependent model accurately calculates the skin effect and the complex propagation characteristics of the XLPE insulation and lead sheaths across a wide frequency band [10].

The simulation was configured with Travel Time Interpolation enabled. Digital EMT simulations calculate data at fixed discrete time steps. Since a travelling wave propagates at high velocity, the true wavefront arrival often falls between two simulation steps. Interpolation allows the solver to estimate the exact arrival instant, preventing discretisation errors that would otherwise compromise the microsecond-level precision required for the fault locator [11].

Table 3.1: Configuration Parameters for PSCAD Frequency-Dependent (Phase) Model

Parameter	Value	Rationale
Curve Fitting Start Freq.	0.5 Hz	Captures low-frequency steady-state behaviour.
Curve Fitting End Freq.	1 MHz	Captures high-frequency fault transients (travelling waves).
Total Freq. Increments	100	Provides sufficient resolution for fitting impedance curves across the wide band.
Maximum Order of Fitting	20	High order required to accurately model the complex impedance of cross-bonded cables.
Travel Time Interpolation	On	Required for accurate wave propagation delay between simulation time steps.

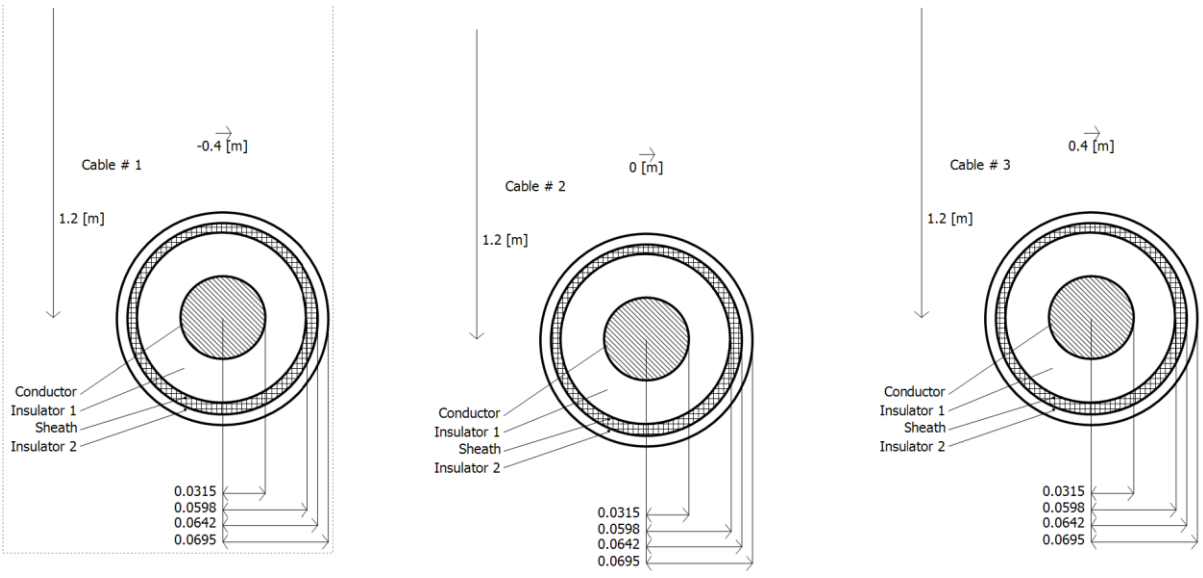

Figure 3.2: Diagram of Cable Trench Layout (Flat Formation)

The physical parameters for the Taihan 400 kV XLPE cable used in the model are derived from the datasheet [13]:

Taihan Cable Parameters

- **Conductor Material:** Aluminium
- **Conductor Cross Section:** 2500 mm2
- **Insulation Material:** XLPE
- **Insulation Thickness:** Nom. 26.0 mm
- **Sheath:** Lead (Pb)
- **Outer Sheath:** High-Density Polyethylene (HDPE)
- **Conductor Resistance (DC at 20 C):** 0.0127 ohm/km
- **Capacitance:** 0.223 uF/km
- **Inductance:** 0.607 mH/km

3.2.2 Tower Modelling and Shunt Reactor Modelling

The overhead lines were modelled using the frequency-dependent geometry of the standard Energinet 400 kV tower [9].

Tower: 3H5
Conductors: AAAC 943

Tower Centre 0.0 [m] →

Ground Wire 1: ACSR Dorking
Ground Wire 2: OPGW

Circuit #	Cond. #	Connection Phasing #	X (from tower centre)	Y (at tower)
	1	1	-12.7 [m]	27 [m]
	2	2	-6.3 [m]	25.5 [m]
	3	3	-6.3 [m]	35.3 [m]

GW. #	Connection Phasing #	X (from tower centre)	Y (at tower)
1	4	-12.7 [m]	42 [m]
2	5	12.7 [m]	42 [m]

Figure 3.3: OHL Tower Geometry

Shunt compensation was provided by fixed shunt reactors at Terminal A (Kassø) and Terminal B (Landerupgård) to neutralise the reactive power generated by the cable capacitance. While physical transition compounds (Arnitlund, Styding, Viuf Vestermark) exist, compensation was aggregated at the line ends to simulate a worst-case scenario for voltage standing waves and to simplify the protection boundary. The reactors were modelled as passive inductive loads connected in a star configuration with a solid ground reference. This topology maintains balanced phase compensation and provides a necessary path for zero-sequence currents during ground faults, replicating the physical installation at the line terminals.

3.2.2 Impedance Mismatch and Reflection Coefficients

With the physical parameters of the cable and overhead line established, the signal behaviour at the impedance boundaries can be quantified. As a travelling wave propagates between media with differing characteristic impedances (OHL and UGC), a portion of the energy is reflected while the remainder is transmitted [7].

The Characteristic Impedance (Z_c) is calculated using Equation (2.3) and the cable parameters derived in Section 3.2.1:

$$Z_{cable} = \text{sqrt}(\frac{0.607*10^{-3}}{0.223*10^{-6}})$$

Using the derived cable parameters (L = 0.607 mH/km, C = 0.223 uF/km), the surge impedance of the cable (Z_{cable}) is 52.2 ohms. Comparing this to a representative OHL surge impedance (Z_{ohl}) of 380 ohms [9], the Reflection Coefficient (K_r) for a wave entering the cable is determined by:

$$K_r = \frac{(Zcable - Zohl)}{(Zcable + Zohl)} \qquad (3.1)$$

$$K_r = \frac{(52.2 - 380)}{(52.2 + 380)} = -0.76$$

Since Z_{cable} is significantly lower than Z_{ohl}, the coefficient is negative, resulting in a voltage inversion at the junction. Consequently, the Transmission Coefficient (K_t), defined as $1 + K_r$, is 0.24. This implies that only 24% of the incident voltage magnitude transmits into the cable section, validating the requirement for high-sensitivity detection equipment. The reflection and transmission coefficients for both propagation directions are summarised in Table 3.2.

Table 3.2: Calculated Reflection and Transmission Coefficients

Transition Direction	Source Medium Impedance	Load Medium Impedance	Reflection Coeff. (K_r)	Transmission Coeff. (K_t)	Physical Implication
OHL to UGC	High 380 ohms	Low 52.2 ohms	-0.76	0.24	Attenuation: Only approx. 24% of the voltage surge transmits into the cable. The remainder is reflected negatively.
UGC to OHL	Low 52.2 ohms	High 380 ohms	+0.76	1.76	The voltage amplitude nearly doubles upon exiting to the OHL, though energy is reflected back into the cable.

3.3 Fault Location Algorithm

The two-terminal travelling wave method relies on detecting the fault-generated transient (surge) as it arrives at the line ends. Unlike active pulse-echo methods, this is a passive technique; the fault itself acts as the transmitter, propagating voltage waves outward in both directions simultaneously [14].

The location is derived from the differential time of arrival (Δt) at Terminal A and Terminal B. The fundamental equation relating distance to time in a uniform medium is:

$$x = \frac{L}{2} + \frac{v * (tA - tB)}{2} \qquad (3.2)$$

Where:

- x is the distance to the fault from Terminal A.
- L is the total length of the line.
- v is the propagation velocity of the travelling wave.
- tA and tB are the absolute arrival times (UTC) of the first wavefront at Terminal A and Terminal B, respectively.

The sensitivity of this equation to time synchronisation errors is high. With a propagation velocity v in high-voltage cables approaching $2.0 * 10^8$ m/s (approx. 200 m/us), the term $(v * \Delta t)/2$ implies that a measurement error of just 1 microsecond (Δt) introduces a location error of approximately 100 metres. This necessitates precision hardware capable of sampling in the MHz range, as discussed further in the hardware requirements in Chapter 5.

3.3.1 Velocity Calibration

Given the hybrid nature of the line, a standard constant velocity cannot be used. To address this, the methodology uses a "System Effective Velocity." This is a calibrated average velocity derived from a known fault event. By rearranging the standard location equation, the effective velocity for the specific line topology can be determined:

$$v = \frac{L - 2x}{tA - tB} \qquad (3.3)$$

This calibrated velocity effectively linearises the travel path, testing the hypothesis that a single weighted velocity is sufficient for accurate fault location even in lines with severe impedance discontinuities.

3.4 Summary

The methodology defined the construction of the high-fidelity electromagnetic transient model in PSCAD. By implementing the Frequency-Dependent (Phase) model, the simulation accounts for the non-linear skin effect and cross-bonding interactions within the XLPE cable sections. Furthermore, the mathematical framework for the “System Effective Velocity” was derived to test the hypothesis that a single calibrated velocity allows for accurate fault location across a heterogeneous medium.

Chapter 4

4. Simulation Results

This chapter presents the data obtained from the PSCAD simulation. Two fault scenarios were simulated to investigate the Two-Terminal Synchronised Travelling Wave method's performance:

- **Scenario 1 (Calibration):** A single-phase-to-ground fault in the first cable section (Arnitlund to Styding).
- **Scenario 2 (Validation):** A single-phase-to-ground fault in the final cable section (Viuf Vestermark to Landerupgård).

4.1 Simulation Fault Parameters

The following fault conditions were applied to the model to generate the transient data:

- **Fault Resistance (Rf):** 0.01 ohm (Solid ground fault).
- **Fault Inception Time:** t = 0.085 s (Voltage peak).
- **Fault Type:** Single-Phase-to-Ground (A-G).

Statistically, single-phase-to-ground faults constitute the majority (approx. 70-80%) of transmission line faults [7]. Furthermore, they present a significant challenge for conventional protection due to potential high fault resistance, making them a fundamental benchmark for validating travelling wave methods.

4.2 Theoretical Propagation Velocity

The theoretical velocities for the individual sections were calculated to provide a baseline for the simulation results.

Overhead Line (OHL)

Assuming a relative permittivity (ε_r) of 1.0 for air [7]: $v_{ohl} = 3.00 * 10^8$ m/s

Underground Cable (UGC)

Using the relative permittivity of XLPE (ε_r approx. 2.3) described in Equation (2.4) [8]:

$$v_{cable} = \frac{c}{\mathrm{sqrt}(\varepsilon r)} \qquad (4.1)$$

$$v_{cable} = \frac{(3.00 * 10^8)}{\mathrm{sqrt}(2.3)}$$

$v_{cable} = 1.97 * 10^8$ m/s

4.3 Scenario 1: Calibration Fault (Arnitlund to Styding)

The fault was placed at a distance of 23.866 km from Terminal A. Physically, this location corresponds to the second cross-bonding joint within the Arnitlund-Styding cable section.

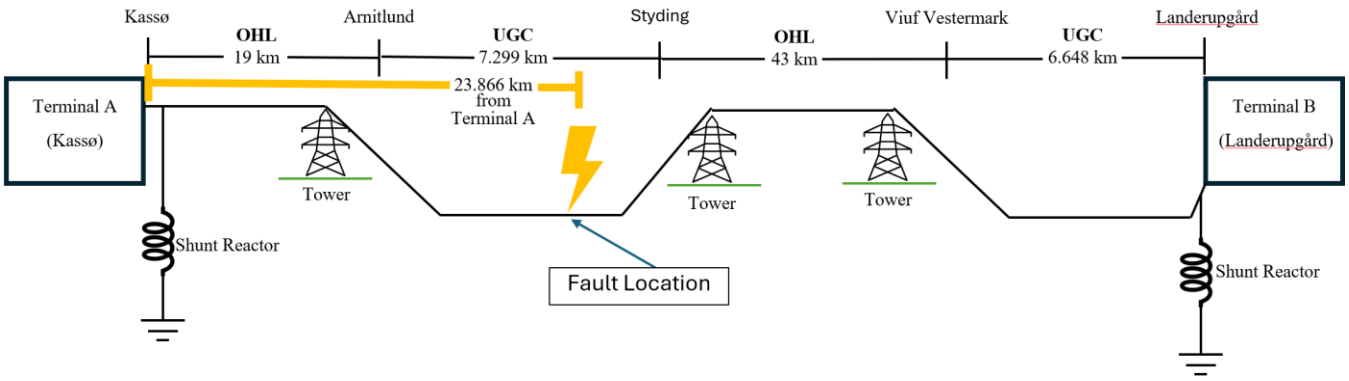

Figure 4.1: Scenario 1 Fault Configuration (Calibration) – Fault at 23.866 km

4.3.1 Terminal Responses

Signal attenuation smoothed the wavefront at Terminal A to the point where no distinct voltage step was visible on the plot. Consequently, the arrival times were determined by inspecting the raw simulation data to identify the exact time step where the voltage value deviated from the pre-fault waveform.

- **Terminal A:** The wavefront arrived at tA = 0.085122 s.
- **Terminal B:** The wavefront arrived at tB = 0.085267 s.

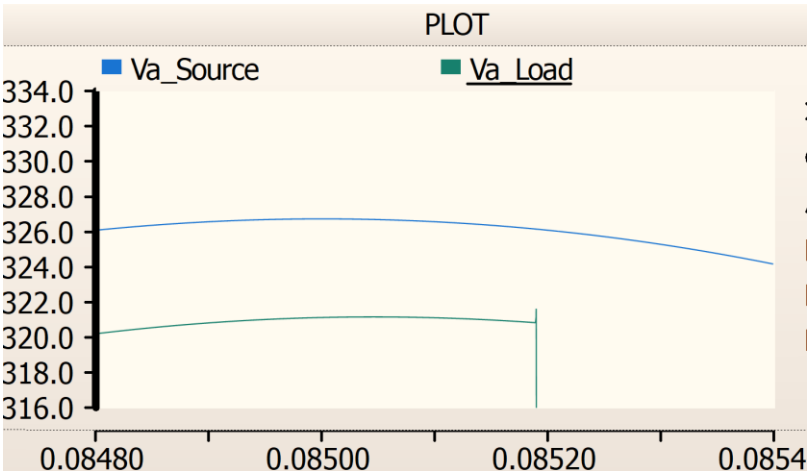

Figure 4.2: Phase A (Faulted Phase) Transient Response during Calibration Fault

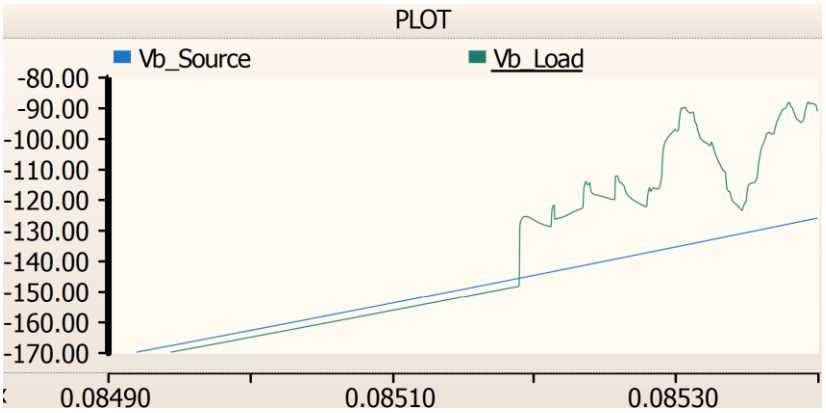

Figure 4.3: Induced Voltage Response on Healthy Phase B during Calibration Fault

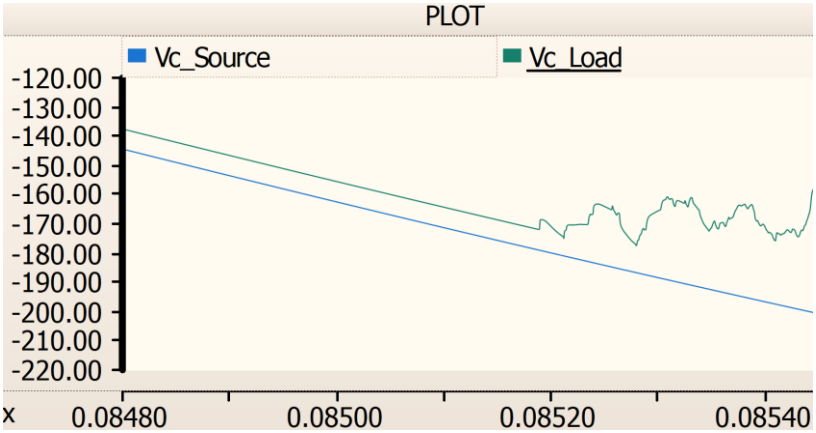

Figure 4.4: Induced Voltage Response on Healthy Phase C during Calibration Fault

4.3.2 Calculation of Time Difference

$\Delta t = tA - tB$

$\Delta t = 0.085122\ s - 0.085267\ s$

$\Delta t = -0.000145\ s$ (-145 microseconds)

4.3.3 Velocity Calibration

Using the known fault location (23.866 km), the effective system velocity was calculated using Equation (3.3):

$$v = \frac{L - 2x}{\Delta t}$$

$$v = \frac{(75947 - 2 * 23866)}{-0.000145}$$

$v = 194{,}586{,}207$ m/s

This magnitude (1.95 * 10^8 m/s) serves as the calibrated velocity for the system. This result correlates closely with the theoretical cable velocity calculated in Section 4.2 (1.97 * 10^8 m/s), validating the PSCAD cable model parameters.

4.4 Scenario 2: Validation Fault (Viuf Vestermark to Landerupgård)

To validate the calibrated velocity, a second fault was initiated in the final cable section, specifically 2.216 km from Terminal B (73.731 km from Terminal A).

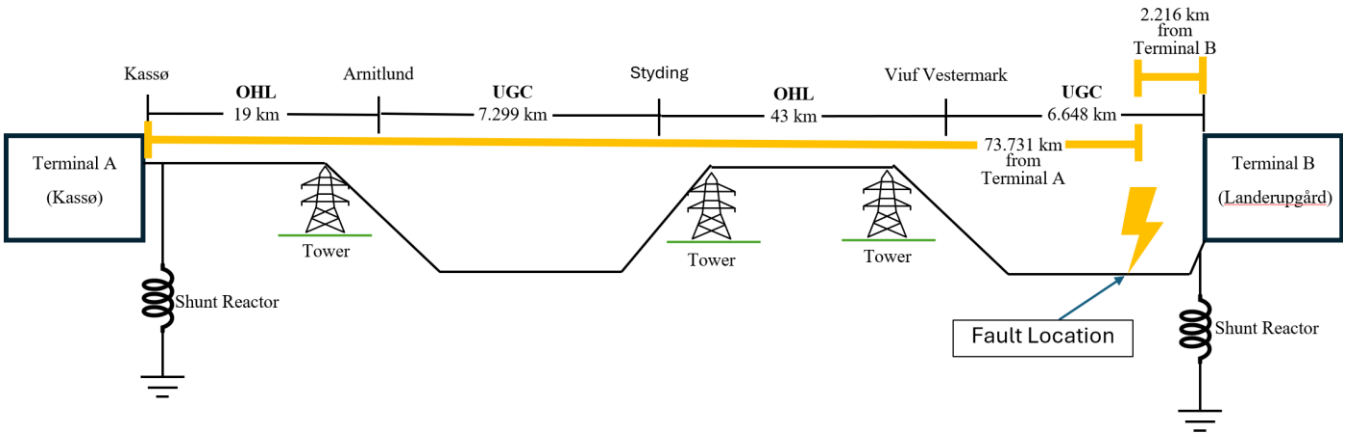

Figure 4.4: Scenario 2 Fault Configuration (Validation) – Fault at 73.731 km

This location creates a propagation path dominated by the central overhead line, providing a rigorous test of the "System Effective Velocity" hypothesis.

4.4.1 Waveform Analysis

Similar to the calibration scenario, signal attenuation smoothed the wavefront at Terminal A to the point where no distinct voltage step was visible on the plot. Consequently, the arrival time tA was determined by inspecting the raw simulation data to identify the exact time step where the voltage value deviated from the pre-fault waveform.

The fault was initiated at t = 0.085 s.

- **Terminal B (Load):** Being in close proximity to the fault (2.2 km), the wavefront arrived almost instantaneously at tB = 0.085011 s.
- **Terminal A (Source):** The wavefront had to travel approximately 73.7 km, traversing two cable sections and the long central overhead line. A local derivative maximum identified the arrival at tA = 0.085355 s.

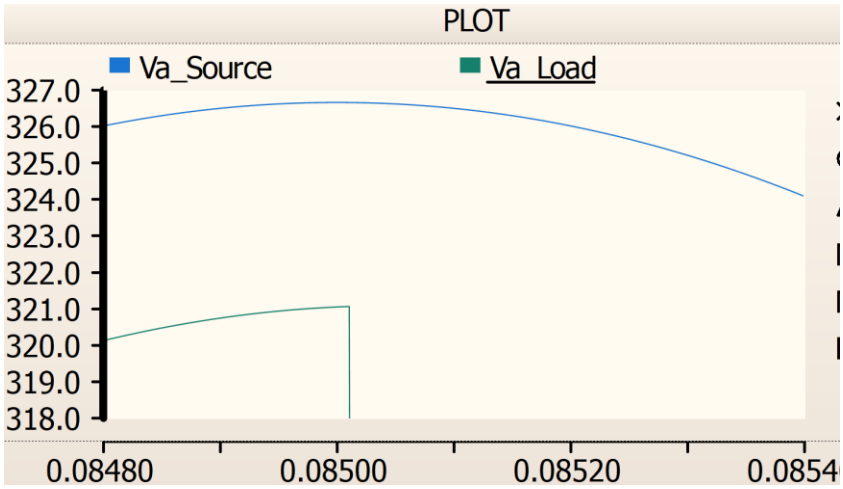

Figure 4.5: Phase A (Faulted Phase) Transient Response during Validation Fault

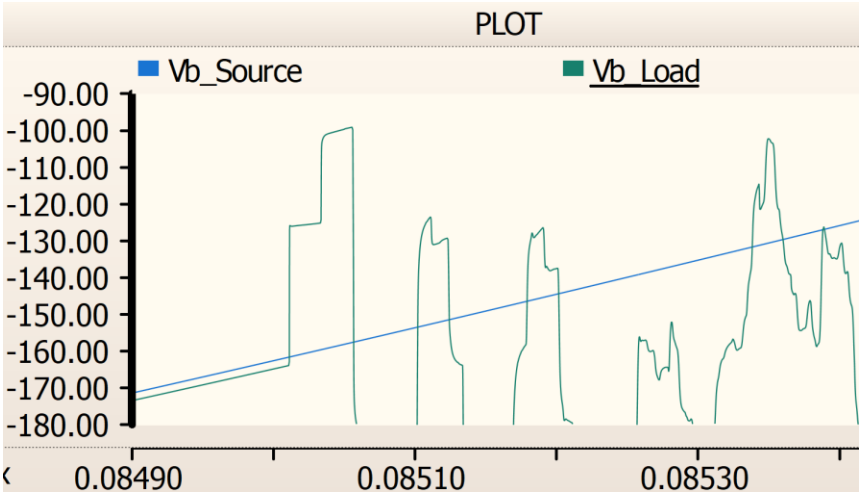

Figure 4.6: Induced Transient Voltage Response on Healthy Phase B during Validation Fault

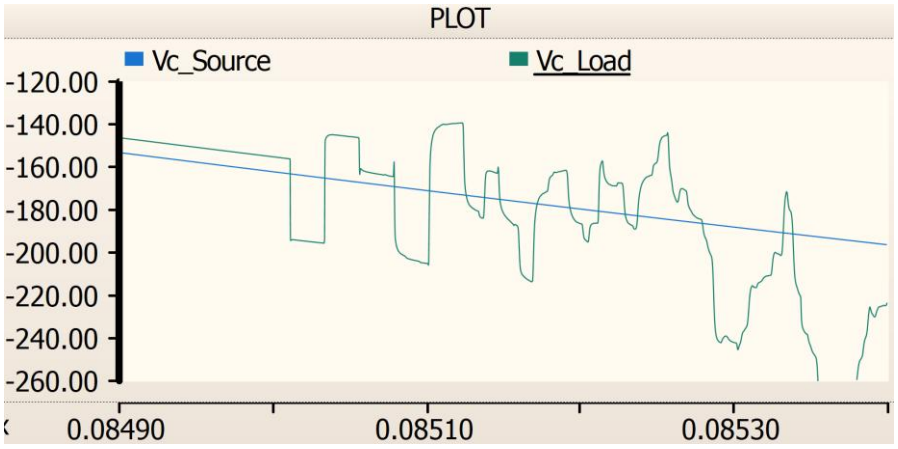

Figure 4.7: Induced Transient Voltage Response on Healthy Phase C during Validation Fault

4.4.2 Location Calculation

First, the differential time of arrival is calculated from the measured timestamps:

$\Delta t = tA - tB$

$\Delta t = 0.085355\ s - 0.085011\ s$

$\Delta t = 0.000344\ s$ (344 microseconds)

Next, the fault location is calculated using the "System Effective Velocity" from Scenario 1,

(v = 194,586,207 m/s) and the total line length (L = 75,947 m).

Applying the travelling wave equation Equation (3.2):

$$x_{calc} = L/2 + \frac{(v * \Delta t)}{2}$$

$$x_{calc} = \frac{75947}{2} + \frac{194586207 * 0.000344}{2}$$

$x_{calc} = 71{,}442$ m

4.4.3 Accuracy Verification

Actual Fault Location: 73,731 m

Calculated Location: 71,442 m

Error: 2.289 km (3.1%)

Table 4.1: Summary of results comparing Actual vs. Calculated fault distance

Scenario	Fault Section	Actual Distance From Terminal A	Calculated Distance From Terminal A	Distance Error (Δx)	Relative Error
1: Calibration	Arnitlund - Styding (UGC)	23,866 m	23,866 m	0 m	0 %
2: Validation	Viuf - Landerupgård (UGC)	73,731 m	71,442 m	(-2,289) m	3.1 %

4.5 Summary

The simulation results demonstrated that the fault-generated transient remains detectable despite the cumulative signal attenuation caused by the transition points. While the "System Effective Velocity" method proved highly accurate (0% error) for the local calibration zone, the validation scenario revealed a dispersion-based error of 3.1% when the wave traversed a significant length of overhead line. This confirms that a single velocity constant is insufficient for remote fault location in hybrid systems.

Chapter 5

5. Discussion and Conclusion

5.1 Discussion of Results

The results demonstrate that while the Two-Terminal Synchronised Travelling Wave method is highly effective, its application to long hybrid OHL-UGC systems introduces complexity regarding propagation velocity.

5.1.1 The Physics of Velocity Mismatch

In Scenario 1, the calibration yielded a velocity of $1.95 * 10^8$ m/s. This velocity accurately represented the specific path from the fault (at 24 km) to the terminals. The wave travelling to Terminal A passed through approximately 19 km of OHL and 5 km of UGC.

However, in Scenario 2, the fault was located at 73.7 km. The wave travelling from this fault back to Terminal A had to traverse a different composition consisting of approximately 62 km of OHL and only 12 km of UGC. The algorithm's error stems from applying the slower cable-weighted velocity to this path, which was predominantly composed of the faster overhead line. Since this propagation path contained a much higher proportion of fast overhead line compared to slow cable, the actual average speed of the wave was higher than the calibrated value ($1.95 * 10^8$ m/s) predicted.

Consequently, as the calculation relied on the slower calibrated velocity, it assumed the wave would take longer to arrive than it actually did. When the wave arrived early due to the high speed of the OHL section, the algorithm interpreted this as the fault being closer to Terminal A, resulting in the under-estimation of distance (71.4 km vs 73.7 km).

This result highlights a significant finding where using a single calibrated velocity produced a 3% error for the remote fault, indicating that the effective velocity is not constant but dependent on the specific path the wave travels from the fault to the terminals.

5.1.2 Implications for Relay Logic

This 3% error demonstrates that a single "System Effective Velocity" is insufficient for precision across a long hybrid line. To achieve the metre-level accuracy desired by Energinet, the relay logic cannot treat the line as a uniform medium. Instead, a "Segment-Based" approach is required. The algorithm must first identify which section (Zone) the fault is likely in, and then apply the specific velocity associated with the OHL or UGC segments in that zone.

Furthermore, the magnitude of this location error observed in Scenario 2 (approx. 2.3 km) poses a significant operational challenge regarding section identification. The transition zones between OHL and UGC are distinct boundaries requiring different repair crews and equipment. Since the single-velocity algorithm resulted in a distance calculation that fell short of the actual fault site, a fault occurring just inside the start of a cable section could be incorrectly identified as occurring in the preceding overhead line section. This misidentification validates the necessity for the segmented logic proposed above, as relying on a single effective velocity could lead to the dispatch of incorrect maintenance teams to the wrong asset type.

5.1.3 Hardware Requirements

The accuracy of this method is highly dependent on the sampling frequency and time synchronisation of the recording devices. In this simulation, the time difference was 145 microseconds. A measurement error of just 1 microsecond would introduce a location error of approximately 100 metres (given the velocity of ~195 m/us). Therefore, implementation in the Energinet grid would require:

1. **High-Speed Acquisition:** Units capable of sampling in the MHz range to capture the steep wavefront.
2. **GPS Synchronisation:** Both terminals must be synchronised via GPS satellites. This technology keeps the clocks at Kassø and Landerupgård locked to within +/– 1 microsecond of Universal Coordinated Time (UTC). Without this external time reference, the clock drift between two independent sub-stations would render the Δt calculation ineffective for accurate fault location [3].

5.2 Conclusion

This thesis investigated the viability of the Two-Terminal Synchronised Travelling Wave fault location for the hybrid Kassø-Landerupgård 400 kV connection. The study modelled the full system in PSCAD, including detailed cable cross-bonding and transition compounds. The validity of the findings is predicated on the use of high-precision recording units capable of MHz-range sampling and microsecond-level GPS synchronisation.

The simulation results indicate that the hybrid nature of the line does not prevent the transmission of the initial fault transient, though significant attenuation occurs over long distances. While a single "Effective Velocity" can be derived for a specific zone, applying this single velocity to the entire hybrid line introduces errors (approx. 3%) due to the varying lengths of OHL and UGC in the fault path. To achieve the highest precision independent of fault location, the protection algorithm must be adaptive, selecting the appropriate velocity based on the zone of the fault.

For the practical application of this system, it is recommended that end-to-end calibration tests be performed not just for one location, but for each distinct section (OHL and UGC) to create a segmented velocity map for the relay logic.

References

[1] Bayati, N., Mortensen, L. K., Savaghebi, M., & Shaker, H. R. (2022). A Localized Transient-based Fault Location Scheme for Distribution Systems. *Sensors*, 22(7), Article 2723. doi: 10.3390/s22072723.

[2] CIGRE Working Group B1.52. (2019). Fault location on land and submarine links (AC & DC) (Technical Brochure 773). CIGRE.

[3] De Almeida, M. J., Lins, H. V., Pires, P. H. S., Pires, T. S. T., & Pinheiro, S. S. (2021). Fault Location in Overhead Transmission Lines Based on Magnetic Signatures and on the Extended Kalman Filter. *IEEE Access*, 9, 15259–15270. doi: 10.1109/ACCESS.2021.3050211.

[4] de Souza, L. M. R. C., Lopes, F. V., Neto, O. M. F., & Pissolato, J. (2021). A Two-Terminal Travelling-Wave-Based Fault-Location Method for Hybrid Transmission Lines. *IEEE Transactions on Power Delivery*, 36(3), 1839-1848. doi: 10.1109/TPWRD.2020.3015556.

[5] El-Saadany, S. M., & El-Kady, M. A. (2019). Analysis of Travelling Wave Propagation at High-Impedance and Low-Impedance Busbars for Fault Location Applications. *IET Generation, Transmission & Distribution*, 13(10), 1935-1943. doi: 10.1049/iet-gtd.2018.6011.

[6] Energinet. (2022). *Cable Action Plan (Kabellægningsplanen)*. Retrieved from https://energinet.dk/

[7] Greenwood, A. (1991). *Electrical Transients in Power Systems*. 2nd Edition. John Wiley & Sons.

[8] Jensen, C. F. (2013). *Online Location of Faults on AC Cables in Underground Transmission Systems*. Aalborg University (PhD Dissertation).

[9] Martinez-Velasco, J. A. (Ed.). (2018). *Power System Transients: Parameter Determination*. CRC Press. doi: 10.1201/9781315200928.

[10] Moradi, A., & Vakilian, M. (2020). Impact of Frequency-Dependent Line Models on Travelling Wave Fault Location Accuracy in PSCAD. *IEEE Transactions on Power Delivery*, 35(4), 1957-1965. doi: 10.1109/TPWRD.2019.2955075.

[11] PSCAD. (2023). *Overhead Lines and Cable Modeling Guidelines for PSCAD*. Retrieved from https://www.pscad.com/knowledge-base/article/872

[12] Rezaee, M., Abdoos, A. A., & Farzinfar, M. (2021). A precise analytical method for fault location in HVAC cables. *Electric Power Systems Research*, 196, 107186. doi: 10.1016/j.epsr.2021.107186.

[13] Taihan Electric Wire Co., Ltd. (2020). *400 kV AC Underground Cable Data Sheet (Lot 1-3)*. Document no. DR310101

[14] Wang, Z., Codino, A., Razzaghi, R., Paolone, M., & Rachidi, F. (2017). Using Electromagnetic Time Reversal to Locate Faults in Transmission Lines. *Physical Review Accelerators and Beams*, 20(9).

[15] Xu, P., Chen, L., Yang, S., Lin, Y., & Dong, X. (2018). Review of the Advanced Fault Location Methods for Transmission Lines Based on Travelling Waves. *Power System Technology*, 42(12), 4887–4896.